

# CONTROL REALLOCATION STRATEGIES FOR DAMAGE ADAPTATION IN TRANSPORT CLASS AIRCRAFT

Karen Gundy-Burlet<sup>\*</sup>  
K. Krishnakumar<sup>†</sup>  
Greg Limes<sup>‡</sup>  
Don Bryant<sup>¶</sup>

## ABSTRACT

This paper examines the feasibility, potential benefits and implementation issues associated with retrofitting a neural-adaptive flight control system (NFCS) to existing transport aircraft, including both cable/hydraulic and fly-by-wire configurations. NFCS uses a neural network based direct adaptive control approach for applying alternate sources of control authority in the presence of damage or failures in order to achieve desired flight control performance. Neural networks are used to provide consistent handling qualities across flight conditions, adapt to changes in aircraft dynamics and make the controller easy to apply when implemented on different aircraft. Full-motion piloted simulation studies were performed on two different transport models: the Boeing 747-400 and the Boeing C-17. Subjects included NASA, Air Force and commercial airline pilots. Results demonstrate the potential for improving handling qualities and significantly increased survivability rates under various simulated failure conditions.

## INTRODUCTION

Design and production of entirely new aircraft models have plummeted over the last few decades due to the high design cycle cost and long development time. Instead, most “new” aircraft are incremental improvements over existing models. While most current transport aircraft have been designed for a thirty-year life cycle, they are often flown long beyond the design lifetime (i.e. the B-52 is now 50 and is anticipated to still fly for approximately another 45 years). No new B-52 airframes are being produced.

---

<sup>\*</sup> Research Scientist, NASA Ames Research Center, Moffett Field, CA. Senior Member, AIAA.

<sup>†</sup> Research Scientist, NASA Ames Research Center, Moffett Field, CA. Associate Fellow, AIAA.

<sup>‡</sup> Computer Engineer, QSS Inc. Ames Research Center, Moffett Field, CA

<sup>¶</sup> Pilot, QSS Inc. Ames Research Center, Moffett Field, CA

Instead, new technologies and mission needs drive the upgrade of specific components. These combined effects mean that if one is to field a neural flight control system on a transport aircraft, one must consider how to retrofit the technology to the existing aircraft designs, rather than rely on a completely new aircraft. While it is conceptually easy to think of software retrofits for fly-by-wire planes, there will continue to be a large number of cable-hydraulic aircraft in the fleet for the next several decades. The natural question is whether it would be useful, possible and/or feasible to incorporate adaptive flight controllers on cable/hydraulic aircraft. Integration issues relative to both classes of aircraft will be discussed in this paper.

The neural network based approach incorporates direct adaptive control with dynamic inversion<sup>1,2</sup> to provide consistent handling qualities without requiring extensive gain-scheduling or explicit system identification. This particular architecture uses both pre-trained and on-line learning neural networks, and reference models to specify desired handling qualities. Several different control allocation techniques have been incorporated, including a-priori daisy chain, a table-driven reallocation technique and a full simplex method linear programming theory reallocation technique.

Piloted simulation studies were performed at NASA Ames Research Center on two different transport aircraft simulators, a Boeing 747-400 and a Boeing C-17. Subjects included NASA and Air Force test pilots and commercial airline pilots. This paper contains a brief overview of the system architecture and presents simulation results comparing the neural-adaptive controller performance to the aircraft’s native control systems under nominal and simulated failure conditions.

## SYSTEM ARCHITECTURE

The neural flight control architecture is based upon the augmented model inversion controller, developed by Rysdyk and Calise.<sup>1</sup> This direct adaptive tracking controller integrates feedback linearization theory with

both pre-trained and on-line learning neural networks. The Integrated Vehicle Modeling Environment<sup>2</sup> is utilized to generate estimates of stability and control derivatives. These derivatives are stored in pre-trained neural networks and are used to provide estimates of aerodynamic stability and control (S&C) characteristics required for model inversion<sup>3</sup> and control allocation. On-line learning neural networks are used to generate command augmentation signals to compensate for errors in the S&C estimates, the model inversion and in the aircraft itself. The on-line learning neural networks also provide additional potential for adapting to changes in aircraft dynamics due to damage or failure. Aircraft reference models are used to filter command inputs in order to specify desired handling qualities. A Lyapunov stability proof guarantees boundedness of the tracking error and network weights.<sup>4</sup> For a detailed discussion of the NFCS algorithm as applied in these studies, please see Kaneshige and Gundy-Burlet<sup>5</sup> and Krishnakumar, et. al<sup>6</sup>

### **CONTROL REALLOCATION STRATEGIES**

Several different control reallocation techniques were utilized in the course of these studies. In the case of a potential retrofit to cable-hydraulic aircraft, it was assumed that significant system upgrades would need to occur for NFCS to be enabled on the aircraft. In particular, the control surfaces on the aircraft would need to be upgraded with systems such as electric ailerons, power by wire systems or the appropriate upgrading with full-authority hydraulic actuators which could use inputs from both the native cable system and the overlaid neural flight control system. To reduce implementation issues, small, isolated integrated sensing/control systems could be applied axis-by-axis in regions localized to the control system (to minimize re-wiring of the aircraft). This concept was designated as NFCS (decoupled). This system has the disadvantage that control requirements in one axis could not be reallocated to surfaces normally utilized to control of other axes.

The second control reallocation scheme utilized a “daisy-chain” approach. In the longitudinal axis, control is provided first by elevators, then symmetric ailerons and spoilers. Lateral control is primarily provided by asymmetric ailerons and spoilers with yaw-based roll control used as a secondary mechanism. Propulsion control<sup>6-8</sup> was not utilized in this experiment because (1) there was no access to the engine FADECs and (2) independently back-driven throttle levers are not currently available on the aircraft or simulators (and would be inordinately expensive to implement). In previous experiments, it was found that the pilot’s situational awareness of the control being utilized is critical to the strategic

maneuvering of the aircraft, and that awareness cannot be adequately provided in propulsion control without back-driven throttles.

The next two control reallocation strategies were implemented only on the fly-by-wire aircraft. One utilized a full simplex method linear programming (LP) theory technique. In this strategy, control derivatives for each axis were estimated for every available control surface on the aircraft and were provided to the LP solver. The dynamic inversion solver was utilized to provide virtual roll, pitch, and yaw commands which were then distributed optimally, according to a cost function, over the available control surfaces. The cost function biased the solution toward the minimum drag configuration and the smallest possible surface deflections to achieve the desired rates. Structural limitations for the subject aircraft are not known, and were not incorporated into the cost function, but the technique admits their potential inclusion in the future.

The final reallocation technique used involved a more complex, but fixed hierarchical schedule table. This table was initially derived by monitoring the solution space of the LP solver. It was hand-tuned to avoid parts of the solution space which we felt would cause structural degradation of the aircraft. It was also felt that the fixed nature of the table would make this technique easier to certify than the full LP solver. These schemes are more rigorously described in Appendix A.

### **TEST ARTICLES AND FACILITIES**

NFCS was evaluated utilizing two separate transport aircraft types in two separate full-motion simulators located at the Crew Vehicle Systems Research Facility (CVSRF) at NASA-Ames Research Center. The first type was a FAA Level-D certified Boeing 747-400 simulator, shown in Figure 1. The second test bed was the Advanced Concepts Flight Simulator (ACFS)<sup>9</sup>, which has been modified to accommodate a model of a Boeing C-17 aircraft. Both simulators are equipped with a six degree-of-freedom motion system, programmable flight displays, digital sound and aural cueing system, and a 180-degree field of view visual system.

The Boeing 747-400 is a cable-hydraulic actuated aircraft with stabilizer, two elevators, four ailerons, twelve spoiler panels and a single rudder, for a total of 20 available control surfaces. For this aircraft, the ailerons and spoilers on each side were ganged together in operation.

The Boeing C-17 is a fly-by-wire transport aircraft with a stabilizer, four elevators, two ailerons, eight

spoiler panels and two rudders, a total of 17 surfaces used for active flight control. Slats, flaps and engines were not used by NFCS for configuration control of either aircraft type. The pilots could manually utilize these surfaces for trim control of the aircraft.



Figure 1. Boeing 747-400 flight simulator.

## **IMPLEMENTATION CONSIDERATIONS**

### **B747-400**

Integration of a fly-by-wire oriented flight control system with a cable-hydraulic airplane such as the Boeing 747 presents difficult issues. Two different implementation concepts were considered. The first would be to independently control the pitch, roll and yaw axis (decoupled option). This could potentially allow distributed processors and sensors located near their primary control effectors (minimizing rewiring of the aircraft). For the decoupled option, it became apparent that if one could retrofit just one axis due to cost or other constraints, retrofitting just the pitch axis offered the greatest single improvement in handling qualities on the plane. In order to allow primary control reallocation to move to unconventional surfaces, the system would need to be fully coupled and would likely require a full fly-by-wire overlay on top of the mechanical system. In either case, the hydraulic actuation systems on the aircraft would need to be retrofitted to full authority systems (for redundancy in case of damage). It was also necessary to postulate hydraulic actuation systems which would accept both mechanical and electronic inputs (or a concept such as power-by-wire and electrically actuated control surfaces<sup>10</sup>).

### **C-17**

The C-17 has a complex spoiler/flap/throttle interconnect system which provides anti-ballooning during configuration changes, speed brake modes (spoilers extend and stay out until commanded to retract) and direct lift control modes (spoilers pop out and back in to finely manage sink rate). These are

essential functions to the C-17 control system and the NFCS command signal had to be overlaid on these signals after the C17 control mixer had operated.

The C-17 has a mechanical backup to the fly-by-wire control system. For transient-free switching, the C-17 SCAS runs continuously (even in mechanical mode), but certain integrators are re-initialized if the flight controller commands are not being utilized. That philosophy was extended for transient-free mode switching between the NFCS and C-17 SCAS controllers. The C-17 SCAS ran in shadow mode even when NFCS was providing commands to the system, but integrators in the SCAS were suppressed to provide transient-free switching between control systems.

One recommendation from the second-generation flight control system study<sup>5</sup> was that the transition from flight to landing and rolling out on the ground needed more study. In that experiment, the neural adaptive flight control system transitioned to a simple gain scheduled system when the wheels touched the ground. This led to hard-to-control transients when the damage adaptive control augmentation suddenly disappeared on touchdown. During the course of this study, it was found that acceptable performance was obtained if:

- NFCS was engaged at rotate speed on takeoff
- NFCS was disengaged when the wheels were on the ground and the plane had decelerated to GO speed.

### **TEST OBJECTIVES**

The purpose of these studies was to evaluate different flight control reallocation techniques and their affect on the handling qualities of the test aircraft. In the case of the Boeing 747, the further intention was to compare the performance of NFCS with the aircraft's native flight control system. The aircraft's normal handling characteristics are shaped by the cable/hydraulic system with yaw dampener (YD) that is intrinsic to the Boeing 747-400 aircraft. For the Boeing C-17, the study was designed to evaluate the combined performance of new control reallocation techniques coupled with adaptive critic reference model adaptation relative to the "daisy-chain" based system utilized in Kaneshige and Gundy-Burlet<sup>5</sup>. The Boeing C-17 implemented in the simulator utilizes an early version of the Boeing stability control and augmentation system, which was not considered sufficiently representative of the control characteristics of the current block-13 aircraft for inclusion in this study.

**B747-400 TEST RESULTS AND DISCUSSION**

The flight control systems were evaluated by a total of 4 pilots (3 NASA test pilots and one commercial airline pilot) on the full-mission motion-based simulator. Pilots evaluated the handling characteristics using the Cooper-Harper (CH) rating scale for maneuvers in high-altitude flight, approach and landing, and take-off scenarios under a range of failure conditions. The test pilots evaluated in-flight handling qualities through a series of pitch and bank maneuvers in nominal conditions and with failures. The failure scenarios included a full tail failure (all surfaces frozen at trim), a coupled stabilizer/rudder failure (stabilizer nose down 3°, rudder 5° offset) and two engines out on one side. Pilot workloads for some cases were increased through addition of moderate turbulence, crosswinds and/or low visibility conditions with an obstructed runway. Table 1 provides specific information on the landing scenarios discussed here.

B747 landing Scenario Number	Scenario Characteristics
1	No Failures, light turbulence, YD
2	No Failures, light turbulence, NFCS/DEC
3	No Failures, moderate turbulence, NFCS/DEC
4	Full Tail Failure, light turbulence, YD
5	Full Tail Failure, light turbulence, runway incursion, NFCS
6	Full Tail Failure, moderate turbulence, NFCS
7	Stab/Rud, light turbulence, Yaw Dampener
8	Stab/Rud, light turbulence, NFCS/DEC
9	Stab/Rud, light turbulence, NFCS/DEC

**Table 1. Landing scenarios for the Boeing 747-400.**  
(YD = Yaw Dampener, DEC = Decoupled axis)

Figure 2 utilizes control column movement as an indication of pilot workload for landing scenarios. The figure displays average absolute deflection and average absolute rate of deflection of the control column in both the roll and pitch axes for a variety of scenarios. The values were then normalized by those obtained in Scenario 1. Three flights were conducted without failures to form a baseline for the rest of the experiment. The pitch deflections for the NFCS scenarios are noticeably reduced relative to the native control system. NFCS provides rate-command, attitude hold (RCAH) capability while the normal cable-hydraulic system must be manually trimmed during flight. The pilots commented that this change provided significant improvement in handling qualities.

In scenarios 4-6, the tail was frozen in the trim position. Only 1 pilot, who had extensive experience with propulsion control, was able to land the un-augmented Boeing 747-400 system. That pilot utilized symmetric and differential engines to control the aircraft, so no stick deflection data is reported here. For cases 5 and 6, NFCS utilized the daisy chain control allocation system, wherein pitch control was obtained through symmetric use ailerons when elevators fail to provide an adequate pitch response. It was found during the course of this experiment, that the inboard ailerons of the 747-400 were insufficient to augment pitch control, so both sets of ailerons were utilized here. Scenario 5 included a low visibility condition in which an aircraft became visible on the runway. At an altitude of 500’ AGL, the pilots were ordered to sidestep to the adjacent runway. Despite the pitch-axis failure, the pitch column deflection was reduced relative to the un-failed cable-hydraulic controller in scenario 1. The pitch column rate was increased over all the un-failed cases, and probably represented additional effort associated with control dead-bands present in the daisy-chain scheme. The pilots all landed safely with the NFCS controller, even when additionally challenged with a runway incursion and sidestep (case 5). It should be noted that without control reallocation of the pitch authority, the NFCS scheme would have provided no significant benefit over the cable-hydraulic system.

In scenarios 7-9, the stabilizer was frozen in a nose-down 3° position and the rudder was frozen at a 5° offset. For the cable-hydraulic system, the pilots all chose to have the copilot manually provide the trim force needed. This is reflected in the pitch column absolute deflection, where on average, the pitch column was deflected about 4 times that of the undamaged cable-hydraulic plane. The pitch column rate was also significantly increased. This represented a significant workload increase and required close coordination between the pilot and copilot. The pilots generally chose to modulate the roll trim to try to minimize wheel trim force, however, it still was significantly greater than for the un-failed case. For cases 8 and 9, NFCS was operated in a decoupled mode. The pitch and roll yoke deflections were significantly reduced over the cable hydraulic system.

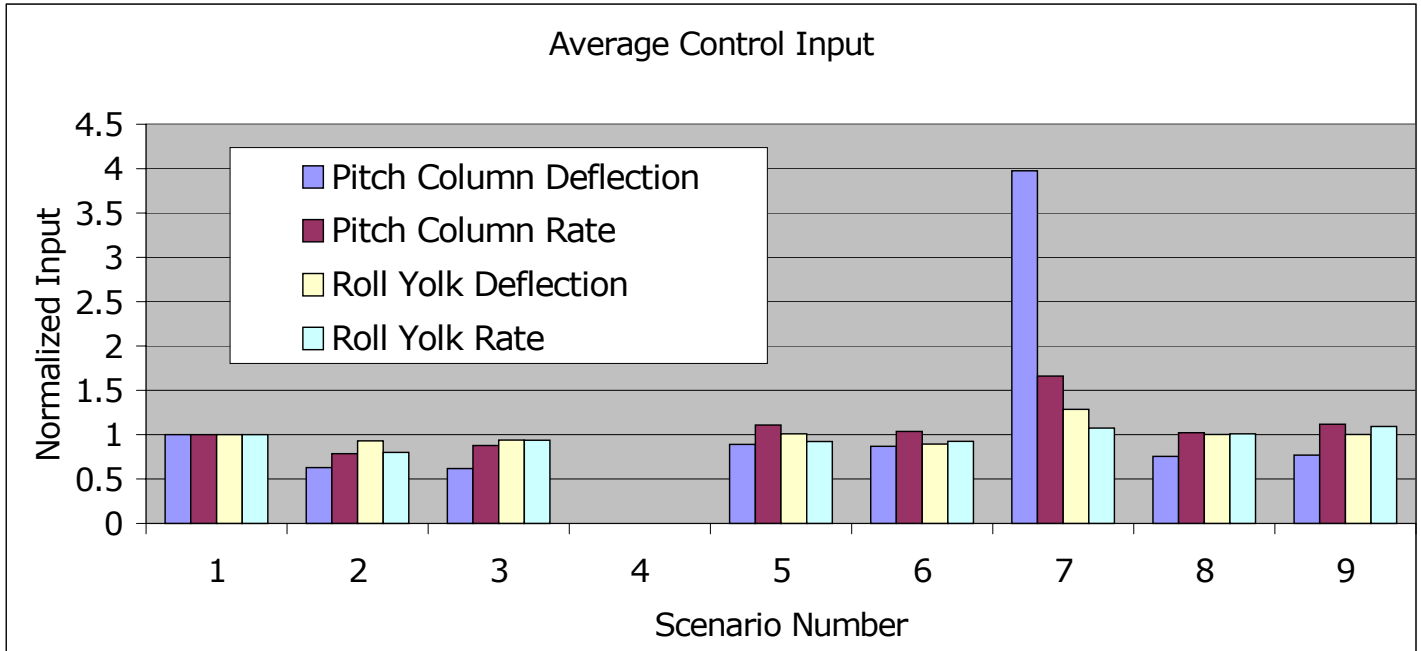


**Figure 2.** Control Column deflection and rate used to indicate pilot workload.

**C-17 TEST RESULTS AND DISCUSSION**

The goal of the C-17 experiment was to evaluate the performance of the third generation control neural flight control systems (LP and table driven reallocation with adaptive critic) relative to that of the second-generation system (daisy chain reallocation). Five C-17 pilots from the Air Force, and NASA were used to compare the second and third generation flight control systems. The native C-17 flight control system was not included in the evaluation because an early version of the flight control system is incorporated in to the simulation, and it was felt that it does not adequately represent the current C-17 SCAS. The evaluation criteria for all the pilots included Cooper-Harper (CH) ratings, approach performance time history data, touchdown snapshot data and pilot comments.

The failure scenarios for the C-17 test are outlined in table 2. The scenarios were designed to test performance of the controllers relative to primary failures in all 3 axes’ as well as a failure sequence which would couple over all the axes. The roll and pitch axis scenarios were utilized during normal landing operations, the yaw axis failure on a takeoff sequence, and the coupled failure during a tactical descent scenario. The pilots were asked to perform handling qualities tests roll, pitch and yaw doublets) during the tests and provide individual CH ratings for each of the three axes.

C17 Scenario	Scenario Characteristics: Winds 190 @ 10, light turbulence
Pitch axis	Full tail failure. Stabilizer failed at trim. 2 rudders, 4 elevators failed at 0 deg.
Roll axis	2 ailerons and 8 spoiler panels failed at 0 deg.
Yaw axis	Two engines out on one side on takeoff, minimum climb speed + 10Kts.
Coupled failure	During tactical descent (failures on one side) 23,000’ : Stab frozen at trim 20,000’ : 2 Elevators frozen at 0 deg. 17,000’ : Upper rudder hard over 15,000’ : Outboard flap fails retracted 14,000’ : Aileron frozen at 0 deg. 13,000’ : Two outboard spoilers frozen at 0 deg. When engines come out of reverse: Outboard engine seizes.

**Table 2.** Failure scenarios for the Boeing C-17 Experiment.

The lateral and longitudinal CH ratings for each of the four scenarios are shown in Figure 3. Heavy horizontal lines indicate the specific pilot ratings. If more than one pilot gave the same rating, the number of pilots giving that rating is listed in Roman Numerals on top of the line. The average CH rating for the pilots is listed above each of the bars on the chart.

CH ratings for the full tail failure scenario for each of the three controllers are shown on the far left columns of the figure. The three controllers are comparable for the longitudinal control, but the table-driven allocator gave more consistent and lower CH ratings than the other two. The Gen-2 controller was optimized for failure of the primary control effectors on the pitch axis. The main complaint about the performance of the Gen-2 controller related to control dead-bands induced by the strict hierarchical daisy chain employed for reallocation. Since there is no explicit system identification utilized, the failed elevators are commanded to their maximum extent and any excess control is passed to symmetric ailerons and spoilers. The LP allocator also utilizes the optimal surfaces first before transitioning to secondary surfaces, thus it has similar dead-bands to the Gen-2 controller (which resulted in similar ratings comments and ratings). The table-driven allocator was designed to minimize control dead-bands. It blends control across surfaces, so that ailerons are utilized for augmenting pitch control much sooner than the other two allocators. This leads to smaller dead-bands and improved CH ratings.

The second scenario involved failure of the primary wing roll control surface (spoilers and ailerons). The daisy chain architecture was designed to utilize yaw-based roll control in response to primary roll control failure. The controller commands the primary roll control surfaces to their maximum extent and then passes excess command to the rudders. The resulting aircraft performance contains a large dead-band, and then utilizes slow aircraft dynamics to achieve roll control. The pilots commented that this made it difficult to make fine tracking adjustments near the ground and gave the controller poor CH ratings in the lateral direction (average 6.6). The LP allocator had similar dead-bands to the daisy chain, but actively used differential elevator and rudder to provide coordinated turns. This gave an improved CH rating over the daisy chain allocation scheme. The table-driven scheme utilized control blending in order to transition roll control to the tail much faster than either of the other schemes. The table was also massaged to limit the severe rudder and elevator deflections that the LP allocator was inducing. This led to smaller dead-bands, but lower control authority for the table-driven allocation scheme and the pilots gave it lower CH ratings (average 5.2) than the other two schemes.

The third scenario involved two engines on one side failing just after take-off at 10,000lb over the theoretical two-engine-out take-off weight. The pilots slightly preferred the table-driven allocation scheme to the other two schemes. The pilots all commented that the workload for all three controllers was distinctly

reduced over the real aircraft (which requires substantial input into the rudder to control the aircraft).

The final scenario was that of a tactical descent while under assault from multiple surface to air missiles. The scenario, described in Table 2, was designed to induce trim offsets and control failures in every axis under high workload conditions. No control dead-bands were induced in this scenario. The table-driven scheme ran out of nose-up control authority during part of the descent requiring a rapid re-configuration of the aircraft to maintain safe flight, which reduced its CH ratings. The LP allocator on average was rated with level I handling qualities while the other two schemes were on average given level II handling qualities.

### **CONCLUSIONS**

The results presented in the previous sections demonstrate the effectiveness of the neural flight control system controlling a transport-class vehicle under a wide range of failure conditions. The generic system can also help to reduce the high cost associated with avionics development since it does not require gain-scheduling or explicit system identification.

In general, the results demonstrate that under normal flight conditions, the neural system can achieve performance, which is comparable to the aircraft's conventional system. The neural flight control system can also provide additional control authority under damaged or failure conditions. For the cable-hydraulic aircraft, significant improvements in handling qualities were provided by the NFCS system, with the pilots advising that primary pitch system augmentation was the most critical. A full retrofit of the aircraft, however, would probably be cost prohibitive.

Results demonstrate that choice of control reallocation technique can significantly improve damage adaptation under various failure conditions. Minimization of dead-bands is key to producing good handling qualities, and should be carefully considered in future research. The pilots generally preferred the table-driven scheme for the simple axis-by-axis failure scenarios with control dead-bands. In the final, highly coupled failure, the pilots generally preferred the LP allocation scheme. This suggests that integration of parameter identification techniques, vehicle health monitoring information or incorporation of control surface blending into the cost function will distinctly improve the handling qualities of the LP allocation scheme, and should be pursued in future research. The results also imply that aircraft structural design must be carefully evaluated when utilizing control surfaces in non-traditional manners.

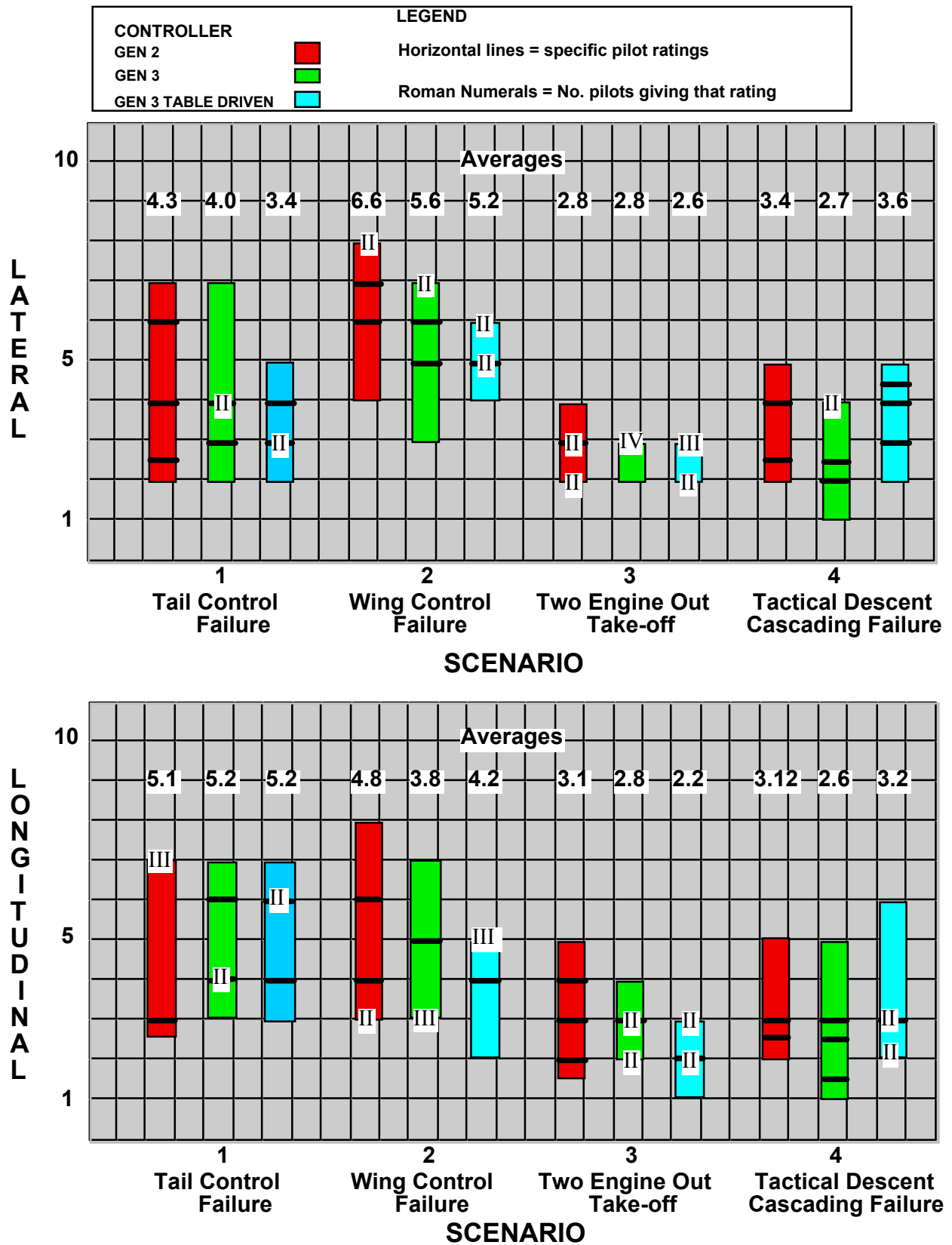


Figure 3. GEN 3 C-17 COOPER HARPER Ratings

### References

- [1] Rysdyk, Rolf T., and Anthony J. Calise, *Fault Tolerant Flight Control via Adaptive Neural Network Augmentation*, AIAA 98-4483, August 1998.
- [2] Totah, Joseph J., David J. Kinney, John T. Kaneshige, and Shane Agabon, *An Integrated Vehicle Modeling Environment*, AIAA 99-4106, August 1999.
- [3] Norgaard, M., Jorgensen, C., and Ross, J., *Neural Network Prediction of New Aircraft Design Coefficients*, NASA TM-112197, May 1997.
- [4] Kim, B., and Calise, A., *Nonlinear Flight Control Using Neural Networks*, AIAA Journal of Guidance, Navigation, and Control, Vol. 20, No. 1, 1997.
- [5] Kaneshige, J. and Gundy-Burlet, K. *Integrated Neural Flight and Propulsion Control System*, AIAA 2001-4386, August 2001.
- [6] KrishnaKumar, K., Limes, G., Gundy-Burlet, K., Bryant, D., *An Adaptive Critic Approach to Reference Model Adaptation*. Accepted to the 2003 AIAA GN&C Conf.
- [7] Kaneshige, J., Bull, J., Kudzia, E., and Burcham, F., *Propulsion Control with Flight Director Guidance as an Emergency Flight Control System*, AIAA 99-3962, August 1999
- [8] Burcham, Frank W., Jr., John J. Burken, Trindel A. Maine, and C. Gordon Fullerton, *Development and Flight Test of an Emergency Flight Control System Using Only Engine Thrust on an MD-11 Transport Airplane*, NASA TP-97-206217, Oct. 1997.
- [9] Blake, Matthew W., *The NASA Advanced Concepts Flight Simulator: A Unique Transport Aircraft Research Environment*, AIAA-96-3518-CP.
- [10] Alden, R. E., *Flight demonstration, evaluation, and proposed applications for all electric flight control actuation concepts*, AIAA 93-1171.



**APPENDIX A –  
CONTROL ALLOCATION TECHNIQUES**

In the material that follows, we outline the three different control allocation techniques used in this study. These are:

- Daisy chain control allocation
- Optimal control allocation using linear programming
- A table-look up with blending

**Daisy Chain**

In the daisy chain approach, secondary control surfaces are used in a hierarchical form to compensate for failures in primary control surfaces. If propulsion control is utilized, the engines become tertiary control effectors. The table below presents the hierarchy. The alternate control sources are used only when the limits of the primary control surfaces are exceeded.

	Elevator	Symmetric Aileron	Differential Aileron	Rudder
Pitch Axis	Primary	Secondary		
Roll Axis			Primary	Secondary
Yaw Axis				Primary

Table A. Daisy Chain Allocation Table

**Optimal Control Allocation**

In optimal control allocation, the choice of the hierarchy is not predetermined as in daisy chain. The choice of alternate surfaces depends on both surface effectiveness and a cost function. The cost function is used to bias the solution toward configurations of interest (i.e. minimum drag). In this section, we present the equations that lead to a problem formulation that is tractable to optimize in real time using linear programming.

The aircraft dynamic system is conveniently defined as:

$$[\dot{X}] = f(X) + [B][u] + f_{trim}$$

Let a portion of the vector  $u$  hit the limit  $u_L$ . We now partition the  $[B][u]$  matrix as follows:

$$\begin{bmatrix} B_{UU} & B_{UL} \\ B_{LU} & B_{LL} \end{bmatrix} \begin{bmatrix} u_U \\ u_L + \Delta u_L \end{bmatrix} = \begin{bmatrix} B_{UU} & B_{UL} \\ B_{LU} & B_{LL} \end{bmatrix} \begin{bmatrix} u_U \\ u_L \end{bmatrix} + \begin{bmatrix} B_{UU} & B_{UL} \\ B_{LU} & B_{LL} \end{bmatrix} \begin{bmatrix} 0 \\ \Delta u_L \end{bmatrix}$$

$u_U$  = vector of UNLIMITED control variables

$u_L + \Delta u_L$  = vector of LIMITED control variables, with  $u_L$  = limit.

To overcome the control needed beyond the limit, defined as  $\Delta u_L$ , we need the unlimited control variables  $u_U$  to compensate by an amount  $\Delta u_U$ . The needed relationship to compute  $\Delta u_U$  is:

$$\begin{bmatrix} B_{UU} \Delta u_U \\ B_{LU} \Delta u_U \end{bmatrix} = \begin{bmatrix} B_{UL} \Delta u_L \\ B_{LL} \Delta u_L \end{bmatrix} \quad (A)$$

Let us now define a control reallocation matrix  $[\lambda]$  such that

$$[\Delta u_U] = [\lambda][\Delta u_L]$$

Substituting the above equation in Equation A, we get

$$\begin{bmatrix} B_{UU} \\ B_{LU} \end{bmatrix} [\lambda] = \begin{bmatrix} B_{UL} \\ B_{LL} \end{bmatrix}$$

For convenience, let us define the above relationship in a compact matrix-vector form as follows:

$$[\alpha][\lambda] = [\beta] \text{ or equivalently}$$

$$[\alpha][\lambda_1 \ \lambda_2 \ \dots \ \lambda_m] = [\beta_1 \ \beta_2 \ \dots \ \beta_m] \quad (B)$$

where

$\lambda_1 \ \lambda_2 \ \dots \ \lambda_m$  are the columns of matrix  $[\lambda]$

$\beta_1 \ \beta_2 \ \dots \ \beta_m$  are the columns of matrix  $[\beta]$

To allocate the available control surfaces optimally, we define the following Linear Programming problem.

$$\min_{w_i} (w_i^T \lambda_i)$$

subject to

$$[\alpha][\lambda_i] = [\beta_i] \quad \text{and} \quad \lambda_{\min} \leq \lambda_{ij} \leq \lambda_{\max}$$

The weighting vector  $w_i$  can be used to effect the preferred choice of control reallocation. For example, to

use ailerons first when elevators saturate, the corresponding elements of  $w$  for ailerons will be small and elements corresponding to other control surfaces will be big.

The optimization problem stated above might not be realizable in cases in which sufficient control authority does not exist after limit violation. A general framework for “standard-LP” based control allocation can now be stated as follows:

$$\min_{w_i} (w_i^T \lambda_i)$$

subject to

$$[\bar{\alpha}] [\lambda_i] \leq [\bar{\beta}_i] \quad \text{and} \quad \lambda_{ij} \geq 0$$

In the above equation,  $[\bar{\beta}_i] = \text{abs}([\beta_i])$  and  $[\bar{\alpha}]$  represents the row elements of  $[\alpha]$  have their signs reversed relative to the sign of the elements in  $[\beta_i]$ .

#### **Control allocation with blending**

One of the problems with adapting to system faults with no explicit fault identification is the time needed for the adaptive element to wind-up the error to drive the failed control surface command to its perceived limit. This “dead band” translates to a degraded handling quality of the aircraft. To alleviate this, one could blend primary and secondary controls just before the perceived surface limit is reached. This can be achieved by defining certain pseudo limits (Figure A) for each of the surfaces to achieve early transition to secondary controls in anticipation of hitting the actual limits. In the next set of equations, we present the equations for implementing the blending for the pitch axis. Similar equations could be derived for roll and yaw axes.

Assumptions:

$$\frac{\partial M}{\partial \delta_e}, \frac{\partial M}{\partial \delta_a} = \text{pitching moment derivatives due to}$$

elevators and ailerons are known (similarly for other axes)

Pseudo limits =  $\delta_{e1}$  are given (similarly for other axes)

Net effective pitch acceleration due to control, after pseudo limit has been hit is computed as:

$$k \frac{\partial M}{\partial \delta_e} \delta_e = \frac{\partial M}{\partial \delta_e} \delta_{e1} + \left[ \alpha \frac{\partial M}{\partial \delta_e} (\delta_e - \delta_{e1}) \right]_{\text{Primary}}$$

$$+ \left[ \beta \frac{\partial M}{\partial \delta_e} (\delta_e - \delta_{e1}) \right]_{\text{Secondary}} \quad (\text{C})$$

To achieve blending, the tunable gains,  $\beta$ ,  $\alpha$ , that are limited to lie between 0 and 1, need to be set. If  $\beta = 0$ ,  $\alpha = 1$ , we get no blending. If  $\beta = (1 - \alpha)$ , we get blending with unity gain ( $k = 1$ ). If  $\beta > (1 - \alpha)$ , we get  $k > 1$  and there is an effect of amplifying the controller gain.

For pitch control, we can compute the aileron needed to blend for the required pitch acceleration using equation C as follows:

$$\frac{\partial M}{\partial \delta_a} \Delta \delta_a = \left[ \beta \frac{\partial M}{\partial \delta_e} (\delta_e - \delta_{e1}) \right]$$

Rearranging, we get

$$\Delta \delta_a = \beta (\delta_e - \delta_{e1}) \frac{\partial M / \partial \delta_e}{\partial M / \partial \delta_a} \quad (\text{D})$$

A look-up table can be constructed for each axis using similar derivations. The entries of the look-up table for blending aileron control for the pitch axis will be the constants  $\beta$ ,  $\delta_{e1}$ , and  $\frac{\partial M / \partial \delta_e}{\partial M / \partial \delta_a}$ .

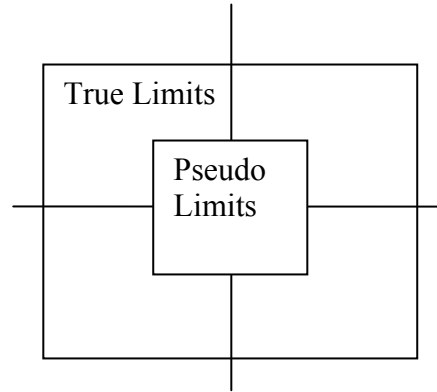


**Figure A.** Notional “Pseudo limits” for minimizing control dead bands.